Dalton Transactions

Cooperative Activation of O-H and S-H Bonds Across the Co-P Bond of an N-heterocyclic Phosphido Complex

Journal:	*Dalton Transactions*
Manuscript ID	DT-ART-12-2018-005052.R1
Article Type:	Paper
Date Submitted by the Author:	05-Feb-2019
Complete List of Authors:	Poitras, Andrew; Ohio State University Department of Chemistry and Biochemistry, Department of Chemistry and Biochemistry Bezpalko, Mark; Villanova University, Chemistry Foxman, Bruce; Brandeis University, Department of Chemistry Thomas, Christine; Ohio State University Department of Chemistry and Biochemistry, Department of Chemistry and Biochemistry

Dalton Transactions

ARTICLE

Cooperative Activation of O-H and S-H Bonds Across the Co-P Bond of an N-heterocyclic Phosphido Complex

Andrew M. Poitras,[a] Mark W. Bezpalko,[b] Bruce M. Foxman,[b] and Christine M. Thomas* [a]

Received 00th January 20xx,
Accepted 00th January 20xx

DOI: 10.1039/x0xx00000x

www.rsc.org/

Metal-ligand cooperation has proven to be a viable concept for σ bond activation and catalysis, however there are few examples involving phosphorus as an active participant in bond cleavage. The reactivity of E-H bonds (E = S, O) across a metal-phosphorus bond of a cobalt(I) center ligated by a tridenate N-heterocyclic phosphido (NHP^-) ligand with diphosphine sidearms, $(PPP)^-$, has been explored. Addition of PhOH to $(PPP)CoPMe_3$ (**1**) cleanly affords $(PP^{OPh}P)Co(H)PMe_3$ (**2**), in which the O-H bond was heterloytically cleaved across the M-P^{NHP} bond. Addition of PhSH to **1** first generates $(PP^{HP}P)Co(SPh)PMe_3$ (**3**), which undergoes an intermolecular rearrangement to generate $(PP^{SPh}P)Co(H)PMe_3$ (**4**) as the thermodynamic product. A comparison with a related platinum(II) system reveals the subtle effects that variations in metal intrinsic properties can have on metal-ligand bifunctional σ bond activation processes.

Introduction

The activation of σ bonds using transition metal complexes is crucial to organometallic chemistry and its applications to organic synthesis and small molecule activation.[1] Transition metal catalysis is typically enabled by the cleavage and formation of σ bonds through oxidative addition and reductive elimination. The majority of transition metal catalysts used industrially or in synthetic laboratories therefore contain precious metals that are able to undergo the two electron redox cycling required for oxidative addition and reductive elimination. Two-electron redox couples are typically less favourable for first row transition metals, making it more challenging to accomplish traditional closed shell oxidative addition / reduction elimination pathways with these more Earth-abundant metals.[2, 3]

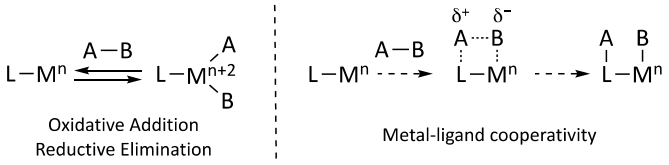

Figure 1. The activation of σ bonds through either oxidative addition/reductive elimination (left) or metal-ligand cooperativity (right) pathways.

A promising approach to enable first row transition metals to promote small molecule activation is to utilize metal-ligand cooperativity. Both bifunctional substrate activation and ligand-assisted redox processes can facilitate the two electron couple.[4-12] For example, A-B bonds can be heterolytically cleaved across a M-L bond (Figure 1), which does not require an oxidation state change on either the metal or ligand. Activation of σ-bonds across metal-element bonds (element = N, O, C, S, B) has become increasingly common in both stoichiometric and catalytic reactions.[4] H-H and E-H (E = heteroatom) bond activation using metal-ligand cooperation has been well-studied studied using metal amide/amine systems, most notably Noyori's catalyst.[13-18] Examples of metal-ligand cooperation that employ phosphorus-based ligands are far less common in the context of H_2 activation.[19-24] The addition of O-H and S-H bonds across metal phosphide linkages has also been reported,[25-29] and Lee and coworkers have reported several interesting examples of reversible intramolecular thiolate and alkoxide migration between a nickel center and a bound phosphide donor in the central position of a bis(phosphino)phosphide pincer ligand.[30-32] Interestingly, Paine and coworkers reported an example of protonation of a $W{=}P(Ph)(N(SiMe_3)_2)$ complex in which initial protonation occurred at the metal center, and subsequent treatment with ancillary ligands prompted migration of the proton to the phosphorus center.[33]

Extending the metal-ligand cooperativity observed with metal amide/amine systems to phosphorus analogues has the potential to lead to enhanced or divergent reactivity patterns owing to their ambiphilic behaviour. Disubstituted phosphorus ligands can be described as either PR_2^- (phosphido) or PR_2^+ (phosphenium) in a fashion similar to the distinction between Fischer and Shrock-type carbenes.[34] The two extremes of the chosen formalism differ by a two-electron change in metal oxidation state and a metal-bound secondary phosphine M-PR_2H could be considered as either acidic or hydridic. Much like N-heterocyclic carbenes, the use of nitrogen substituents and incorporation into a heterocyclic framework stabilizes N-

[a] Department of Chemistry and Biochemistry, The Ohio State University, 100 West 18th Avenue, Columbus, Ohio 43210, United States
[b] Department of Chemistry, Brandeis University, 415 South Street, Waltham, Massachusetts 02453, United States

Electronic Supplementary Information (ESI) available: Spectroscopic characterization data for **2**-**4**, crystallographic data collection and refinement details for **2**, computational details, and XYZ coordinates of optimized geometries for **2**-**4**. CCDC 1876919. See DOI: 10.1039/x0xx00000x

heterocyclic phosphenium cations (NHP^+s) in the singlet form.[34-39] However, recent work by our group has shown that incorporation of the NHP^+ moiety into a rigid pincer ligand framework enforces a pyramidal geometry about the phosphorus atom when bound to an electron-rich transition metal, leading to a ligand that is better described as a formally reduced N-heterocyclic phosphide (NHP^-).[40-43] Both the NHP^+ and NHP^- forms have the respective electrophilic and nucleophilic properties to potentially participate in metal-ligand bifunctional σ bond activation. For example, Gudat and coworkers reported that treatment of $Na[(NHP^{Dipp})Fe(CO)_3]$ with MeI results in addition of the Me^+ electrophile to the NHP phosphorus atom,[44] while addition of $Li[BEt_3H]$ to $(NHP^{Dipp})Mn(CO)_4$ results in nucleophilic addition of H^- to the NHP phosphorus atom (where NHP^R indicates a monodentate NHP^+ cation with N-R substituents and Dipp = 2,6-diisopropylphenyl).[45] The same group also recently demonstrated that $(NHP^{Dipp})Mn(CO)_4$ is an active catalyst for the catalytic dehydrogenation of H_3NBH_3.[45]

In this context, our group has been actively exploring transition metal complexes of a pincer ligand with a central $NHP^{+/-}$ moiety, $(PPP)^{+/-}$,[46] and their ability to activate σ bonds across the metal-phosphorus bond through metal-ligand cooperative pathways. In a previous work, we demonstrated that the Pt^{II} NHP^- complex, $[(PPP)PtPPh_3]PF_6$, is able to heterolytically cleave polar E-H bonds (E = S, O, Cl) across the Pt-P^{NHP} bond to afford new Pt^{II} complexes containing functionalized N-heterocyclic phosphine/phosphinito species such as $[(PP^HP)Pt(SPh)][PF_6]$ and $[(PP^{OPh}P)Pt(H)PPh_3][PF_6]$.[47] Upon extension of the coordination chemistry of the $(PPP)^-$ ligand to cobalt, we found that the Co^I/NHP^- complex $(PPP)CoPMe_3$ (**1**), activates H_2 across the Co-P^{NHP} bond to afford new Co-H and P-H bonds in $(PP^HP)Co(H)PMe_3$.[19] Herein, we further explore the role of the $NHP^{+/-}$-diphosphine pincer ligand in metal-ligand cooperativity and find that complex **1** is also able to heterolytically cleave polar E-H bonds (E = S, O) via 1,2-addition across the Co-P^{NHP} bond.

Scheme 1.

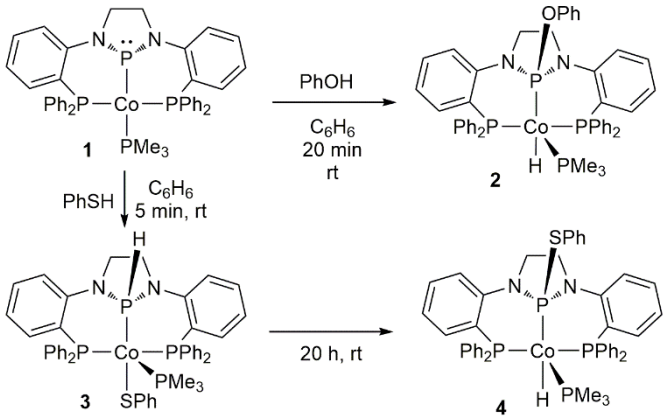

Results and Discussion

To build upon the successful activation of H_2 across the polar Co-P^{NHP} bond of complex **1**,[19] the reactivity of **1** with polar phenolic O-H bonds was explored, anticipating a more facile reaction. Treatment of complex **1** with one equivalent of PhOH at room temperature for 20 minutes resulted in a dramatic color change from dark green to red. The $^{31}P\{^1H\}$ NMR spectrum of the resulting red solution revealed new resonances at 152.8, 44.2, and 1.7 ppm, corresponding to the central NHP-derived phosphorus center, two equivalent phosphine sidearms, and a Co-bound PMe_3 ligand, respectively. The upfield chemical shift of the central phosphorus resonance compared to **1** (251 ppm) and the presence of a cobalt-hydride resonance in the ^1H NMR spectrum at -11.8 ppm suggested that the phenolic O-H bond had added across the Co-P^{NHP} bond to generate $(PP^{OPh}P)Co(H)PMe_3$ (**2**, Scheme 1).

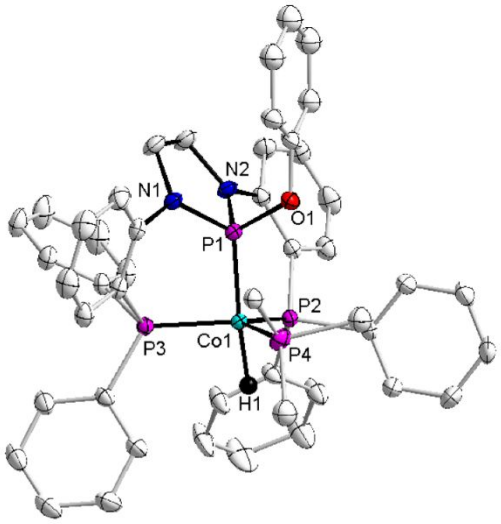

Figure 2. Displacement ellipsoid (50%) representation of **2**. For clarity, all H atoms except for the hydride and solvate molecules have been omitted. The PMe_3 methyl groups, phenoxide Ph ring, and one of the phosphine-bound Ph groups are disordered, but only one position is shown for clarity (see ESI). Relevant interatomic distances (Å): Co1-P1, 2.0393(5); Co1-P2, 2.1070(5); Co1-P3, 2.1300(5); Co-P4, 2.1502(5); Co1-H1, 1.47(3); P1-O1, 1.6631(13); P1-N1, 1.6776(16); P1-N2, 1.6915(16).

The solid-state structure of **2** was determined by single crystal X-ray diffraction, confirming the cleavage of the O-H bond across the Co-P^{NHP} bond (Figure 2). The geometry about the Co center is approximately trigonal bipyramidal ($\tau_5 = 0.84$)[48] with the NHP-derived heterocycle and the hydride occupying the axial positions. The geometry of **2** is similar to $[(PP^{OPh}P)Pt(H)PPh_3][PF_6]$, the previously reported product of the reaction of PhOH with $[(PPP)PtPPh_3][PF_6]$.[47] The Co-P^{NHP} distance (2.0393(5) Å) is significantly shorter than the Co-P^{NHP} distance seen in $(PPP)Co(CO)_2$ (2.2398(6) Å).[40] The Co-P^{NHP} distance in **2** is also contracted compared to the Co-P distances associated with the phosphine ligands (Co-P2: 2.1070(5) Å, Co-P3: 2.1300(5) Å, Co-P4: 2.1502(5) Å), which can be attributed to the three heteroatom substituents that render the N-heterocyclic phosphinite a strong π-acceptor. The DFT-optimized geometry of **2** was found to be 10 kcal/mol lower in energy than the other possible regioisomer $(PP^HP)Co(OPh)PMe_3$

(**2***, see ESI), which is consistent with literature examples of O-H bond heterolysis across M=PR_2 bonds,[27-29] and can be attributed to the oxophilic nature of the phosphorus center.

The reaction of **1** with thiophenol was also investigated, anticipating an analogous S-H bond activation product. Similar to the PhOH reaction, treatment of complex **1** with PhSH at room temperature resulted in an immediate color change from dark green to red. The initial $^{31}P\{^1H\}$ NMR spectrum contained new resonances at 120.9, 32.2, and -22.9 ppm, corresponding to the central NHP-derived phosphorus center, a single resonance for two equivalent phosphine sidearms, and a resonance for bound PMe_3, respectively. In the ^{31}P NMR spectrum, the P^{NHP} resonance splits into a doublet with a large $^1J_{H\text{-}P}$ coupling constant (399 Hz), indicating the formation of a P-H bond. The absence of a hydride resonance in the ^1H NMR spectrum, combined with the ^{31}P NMR data suggested that the S-H bond had added across the Co-P^{NHP} bond to generate (PP^HP)Co(SPh)PMe_3 (**3**, Scheme 1). When the reaction was stirred overnight at room temperature, new $^{31}P\{^1H\}$ NMR resonances grew in at 159.6, 42.2, and -1.7 ppm, corresponding to the central NHP-derived phosphorus center, two equivalent phosphine sidearms, and a Co-bound PMe_3 ligand, respectively. In contrast to the initial product **3**, the central NHP resonance of the new product no longer split into a doublet in the ^{31}P NMR spectrum, signifying that the P-H bond was no longer present. In addition, a new metal hydride signal appeared in the ^1H NMR spectrum at -12.4 ppm, indicating that the Co- and P-bound moieties had switched positions to generate ($PP^{SPh}P$)Co(H)PMe_3 (**4**) over time at room temperature (Scheme 1).

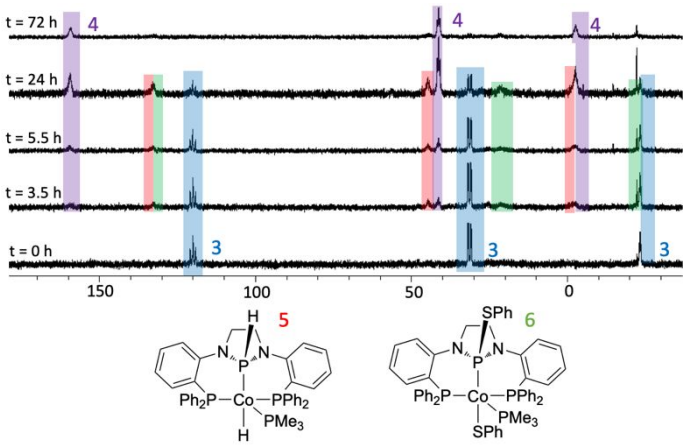

Figure 3. $^{31}P\{^1H\}$ NMR spectra collected after 0, 3, 6, 24, and 72 h while monitoring the reaction between 1 and PhSH and subsequent conversion from **3** to **4**. Reaction conditions: 1.0 equiv PhSH, 0.5 mL of C_6D_6, room temperature, in NMR tube without stirring.

To further probe the PhS/H exchange process that occurs during the conversion of **3** to **4**, the progress of the reaction was monitored by $^{31}P\{^1H\}$ NMR spectroscopy. These reactions were performed in C_6D_6 at room temperature and initially monitored every 3 hours, then every 24 hours until completion. When performed in NMR tubes without stirring, the reactions proceed significantly slower, allowing the observation and identification of intermediates (Figure 3). While monitoring the reactions by $^{31}P\{^1H\}$ NMR spectroscopy, two intermediates were observed with overlapping P^{NHP} resonances between 131-136 ppm, sidearm resonances at 46 ppm and 22 ppm, and PMe_3 resonances that overlap with the signals of **3** and **4**. In the ^1H NMR spectrum an additional metal hydride peak was observed at -11 ppm. Based on a comparison with previously reported NMR data,[19] the $^{31}P\{^1H\}$ NMR resonances at 134, 46, and -0.1 ppm and the additional ^1H NMR hydride signal were assigned to (PP^HP)Co(H)PMe_3 (**5**). The second intermediate is hypothesised to be ($PP^{SPh}P$)Co(SPh)PMe_3 (**6**, Figure 3), although attempts to synthesize and isolate this compound independently have been unsuccessful. The generation of intermediates **5** and **6** suggest that the conversion of **3** to **4** is intermolecular in nature, rather than a concerted intramolecular rearrangement.

To further probe the mechanism, the concentration dependence of the conversion of **3** to **4** was investigated. A 63 mM solution of **3** converted to 65% of **4** in 96 h, while a more dilute 6.5 mM solution proceeded to only 14% conversion in the same timeframe (96 h), which indicates an intermolecular process. The impact of excess PhSH on the rate of conversion from **3** to **4** was also investigated. The addition of six equivalents of PhSH to **1** initially generated **3**, which subsequently underwent much more rapid conversion to **4**, reaching completion in 31 h vs 72 h with 1 equiv PhSH. Conversely, the addition of 0.5 equivalents of PhSH to **1** generated a 50:50 mixture of unreacted **1** and **3**, which converted to **4** at a significantly slower rate, reaching only 60% conversion over 244 hours; the unreacted **1** in this mixture remained unchanged. Both intermediates (**5** and **6**) were observed in the reaction with substoichiometric PhSH, but not when excess PhSH was used. Moreover, it was found that the cobalt-bound thiolate in **3** readily exchanges with that of free thiol: Generation of **3** in situ with one equiv PhSH, followed by addition of 3,5-dimethylbenzenethiol afforded a 50:50 mixture of **3** and (PP^HP)Co(SAr)PMe_3 (**3'**, Figure S9). Therefore, the conversion between **3** and **4** appears to be mediated by exchange with free PhSH, although the exact mechanism remains unclear.

Although crystals of **3** and **4** suitable for X-Ray diffraction could not be obtained, the diamagnetism of these complexes allows for reliable assignment of their formulation and connectivity using NMR spectroscopy. DFT calculations were also used to predict the geometric configurations and relative energy differences between **3** and **4**. The DFT-optimized structure of **4** is similar to that of **2** and features a distorted trigonal bipyramidal geometry (τ_5 = 0.78).[48] Complex **4** was found to be 4 kcal/mol lower in energy than **3** (Table S6), consistent with the initial formation of **3** and the eventual conversion to **4** as the thermodynamic product.

Comparing the products formed from the PhOH and PhSH activation reactions of complex **1** and the previously reported Pt analogue [(PPP)$PtPPh_3$][PF_6], we find that activation of the O-H bond generates similar products, ($PP^{OPh}P$)Co(H)PMe_3 (**2**) and [($PP^{OPh}P$)Pt(H)PPh_3][PF_6], due to the oxophilic nature of phosphorus.[47, 49] However, the reaction of PhOH with **1** occurs readily at room temperature and is much more facile compared

to reaction with the Pt analogue, which requires several days at elevated temperature to proceed. The kinetic product of the reaction of PhSH with **1** is also similar to the previously reported product from the Pt study, (PP^HP)Co(SPh)(PMe_3) (**3**) vs [(PP^HP)Pt(SPh)][PF_6], although one notable difference is that the ancillary phosphine ligand remains bound to Co while PPh_3 dissociation occurred in the Pt case. The Pt and Co complexes differ, however, in that the Co complex **3** undergoes a thermodynamically driven isomerization process to generate P-SPh/Co-H product **4**, which is ~4 kcal/mol lower in energy than **3**. The P-SPh/Pt-H product was also predicted to be lower in energy than the observed P-H/Pt-SPh product.[47] However, in the Pt case no conversion to [($PP^{SPh}P$)Pt(H)][PF_6] was observed, which indicates a higher kinetic barrier between these two isomers. The difference in products is likely due to hard-soft acid/base preferences, where better orbital overlap of the thiolate group with Pt compared to Co favors the Pt thiolate product.

Conclusions.

In summary, we have shown that the E-H bonds of phenol and thiophenol readily add across the Co-P^{NHP} bond of an N-heterocyclic phosphide complex via 1,2-addition, which is the first example of this type of metal-phosphorus ligand cooperativity involving a first-row metal. In all cases, the oxidation state of the Co center remains the same, illustrating the non-innocent nature of the $NHP^{+/-}$ moiety. The 1,2-addition of the O-H bond of PhOH to the Co-P^{NHP} bond exclusively generates the Co-H/P-OPh product. However, 1,2-addition of the S-H bond of PhSH initially generates the Co-SPh/P-H product, which then undergoes an intermolecular rearrangement to form the more thermodynamically stable Co-H/P-SPh product. Successful E-H bond activation across the M-P^{NHP} bond expands the scope of metal-ligand cooperation with phosphorus and suggests the potential for future catalytic applications.

Experimental.

General Considerations.

Unless otherwise noted, all manipulations were carried out under an inert atmosphere using a nitrogen-filled glovebox or standard Schlenk techniques. Glassware was oven-dried before use. Pentane, tetrahydrofuran, toluene, and benzene were degassed by sparging with ultra-high purity argon and dried via passage through columns of drying agents using a Seca solvent purification system from Pure Process Technologies. Benzene-d_6 was degassed via repeated freeze-pump-thaw cycles and dried over 3 Å molecular sieves before use. (PPP)$CoPMe_3$ (**1**) was synthesized according to literature procedures.[19] Phenol was purified by sublimation at ambient temperature. Thiophenol was purified by drying over CaH_2 for two days, followed by vacuum transferring to an oven-dried vessel. Dry thiophenol was then degassed via repeated freeze pump-thaw cycles and stored over 3 Å molecular sieves. All other reagents and solvents were obtained from commercial sources and used without further purification. NMR spectra were recorded at ambient temperature unless otherwise stated on a Varian Inova, Varian MR, or Bruker DPX 400 MHz instrument. ^1H and ^{13}C NMR chemical shifts were referenced to residual solvent resonances and are reported in ppm. ^{31}P NMR chemical shifts (in ppm) were referenced using an external standard (85% H_3PO_4, 0 ppm). Elemental microanalyses were performed by either Complete Analysis Laboratories, Inc., Parsippany, NJ or Midwest Microlab, Indianapolis, IN.

Synthesis of ($PP^{OPh}P$)Co(H)PMe_3 (2).

Complex **1** (0.048 g, 0.064 mmol) was dissolved in benzene (3 ml). A solution of phenol (0.0068 g, 0.072 mmol) in benzene (1 mL) was added dropwise to the stirring solution of **1**. The resulting red solution was stirred at room temperature for 20 minutes. The solution was filtered through Celite and the solvent was removed from the filtrate *in vacuo* to yield a red/orange oil. The crude red/orange oil was dissolved in benzene (2 mL) and filtered through Celite and the solvent was removed from the filtrate *in vacuo* to yield **2** as a pure red/orange powder (94%, 0.051 g). Red crystals suitable for X-Ray diffraction were grown via vapor diffusion of *n*-pentane into a concentrated toluene solution. ^1H NMR (400 MHz, C_6D_6): δ 7.95 (s, Ar-H, 4H), 7.72 (s, Ar-H, 4H), 7.53 (s, Ar-H, 3H), 7.13 (m, overlapping with C_6D_5H, Ar-H, 2H) 6.95-7.09 (m, Ar-H, 8H), 6.89 (m, Ar-H, 2H), 6.86 (s, Ar-H, 6H), 6.77 (m, Ar-H, 4H), 2.98 (s, CH_2, 2H), 2.29 (s, CH_2, 2H), 1.05 (d, PMe_3, $^2J_{H\text{-}P}$ = 6.2 Hz, 9H), -11.82 (ddt, Co-H, $^2J_{P\text{-}H}$ = 105.4 Hz, 60.0 Hz, 42.4 Hz, 1H). $^{31}P\{^1H\}$ NMR (161.8 MHz, C_6D_6): δ 152.8 (Br m, P^{NHP}, 1P), 44.2 (dd, PPh_2, $^2J_{P\text{-}P}$ = 79 Hz, 2P), 1.7 (br m, PMe_3, 1P). $^{13}C\{^1H\}$ NMR (100.5 MHz, C_6D_6): δ 154.9 (m, $J_{C\text{-}P}$ = 18.1 Hz) , 149.0 (m), 143.0-144.1 (two overlapping m), 134.1 (two overlapping d, $J_{C\text{-}P}$ = 7.2 Hz), 133.6 (s), 133.4 (two overlapping d, $J_{C\text{-}P}$ = 6.9 Hz), 129.6 (s), 129.6 (s), 128.0 (m, overlapping with C_6D_6), 127.2 (two overlapping d, $J_{C\text{-}P}$ = 4.5 Hz), 123.7 (s), 123.0 (d, $J_{C\text{-}P}$ = 2.6 Hz), 121.3 (s), 120.6 (s), 47.3 (d, $J_{C\text{-}P}$ = 4.8 Hz, CH_2CH_2), 23.8 (dm, $J_{C\text{-}P}$ = 20.9 Hz, $P(CH_3)_3$). Anal. Calcd for $C_{47}H_{47}CoN_2OP_4$: C, 67.31; H, 5.65; N, 3.34. Found: C, 67.57; H, 5.83: N, 2.72.

Synthesis of (PP^HP)Co(SPh)PMe_3 (3).

Complex **1** (0.061 g, 0.081 mmol) was dissolved in benzene (3 mL). Thiophenol (8.4 µL, 0.081 mmol) was added directly to the stirring solution of **1**. The resulting red/orange solution was stirred at room temperature for 2 minutes. The solution was filtered through Celite and the solvent was removed from the filtrate in vacuo to yield **3** as a red orange solid (0.042 g, 90%). 1H NMR (400 MHz, C_6D_6): δ 7.84 (s, Ar-H, 6H), 7.10 (s, Ar-H, overlaps with solvent peak), 7.01 (s, Ar-H, 5H), 6.96 (m, Ar-H, 4H), 6.88 (m, Ar-H, 4H), 6.79 (m, Ar-H, 1H), 6.69(m, Ar-H, 2H), 6.53 (m, Ar-H, 2H), 6.47 (m, Ar-H, 2H), 3.17 (br s,CH_2, 2H), 2.70 (br s, CH_2, 2H), 0.91 (br s, PMe_3, 9H). $^{31}P\{^1H\}$ NMR (161.8 MHz, C_6D_6): δ 120.1 (t, P^{NHP}, $^2J_{PNHP\text{-}PPh2}$ = 141 Hz, 1P), 32.2 (dd, PPh_2, $^2J_{PNHP\text{-}PPh2}$ = 139 Hz, $^2J_{PPh2\text{-}PMe3}$ = 39 Hz, 2P), -22.9 (t, $^2J_{PMe3\text{-}PPh2}$ = 39 Hz, PMe_3,1P). ^{31}P NMR (161.8 MHz, C_6D_6): δ 120.1 (dt, $^1J_{P\text{-}H}$ = 399 Hz, $^2J_{PNHP\text{-}PPh2}$ = 141 Hz, P^{NHP}, 1P) 32.2 (dd, PPh_2, $^2J_{PNHP\text{-}PPh2}$ = 139

Hz, $J_{PPh2\text{-}PMe3}$ = 39 Hz, 2P), -22.9 (t, $^2J_{PMe3\text{-}PPh2}$ = 39 Hz, PMe_3, 1P). CHN analysis was not performed since the values would be identical **4**. Owing to the conversion of **3** to **4** in solution, a ^{13}C NMR spectrum was not performed.

Synthesis of ($PP^{SPh}P$)Co(H)PMe_3 (4).

Complex **1** (0.061 g, 0.081 mmol) was dissolved in benzene (3 mL). Thiophenol (8.4 µL, 0.081 mmol) was added directly to the stirring solution of **1**. The resulting red solution was stirred at room temperature for 20 h. The red solution was filtered through Celite and the solvent was removed from the filtrate *in vacuo*. The crude red oil was dissolved in benzene and filtered through Celite and solvent was removed from the filtrate *in vacuo*, affording **4** as a red powder (0.058 g, 83%). ^1H NMR (400 MHz, C_6D_6): δ 8.01 (s, Ar-H, 4H), 7.60 (s, Ar-H, 4H), 7.51 (s, Ar-H, 4H), 7.06 (m, Ar-H, 3H), 6.95 (m, Ar-H, 6H), 6.82 (m, Ar-H, 12H), 2.99 (s, CH_2, 2H), 2.18 (s, CH_2, 2H), 1.09 (d, $^2J_{P\text{-}H}$ = 6.5 Hz, PMe_3, 9H), -12.37 (ddt, Co-H, $^2J_{P\text{-}H}$ = 105.6 Hz, 62.2 Hz, 41.6 Hz, 1H). $^{31}P\{^1H\}$ NMR (161.8 MHz, C_6D_6): δ 159.6 (br s, P^{NHP}, 1P), 42.2 (t, PPh_2, $^2J_{PNHP\text{-}PPh2}$ = 77Hz, 2P), -1.7 (br s, PMe_3, 1P). $^{13}C\{^1H\}$ NMR (100.5 MHz, C_6D_6): δ 148.2 (m), 142.5-143.5 (two overlapping m), 136.2 (m), 136.1 (s), 133.8-133.5 (three overlapping m,), 129.7 (s), 128.7 (s), 128.6 (s) 127.9 (s), 127.5 (s), 127.2 (two overlapping d, $J_{C\text{-}P}$ = 4.4 Hz), 121.5 (s), 121.2 (s), 47.3 (d, $J_{C\text{-}P}$ = 4.74 Hz, CH_2CH_2), 24.4 (dm, $J_{C\text{-}P}$ = 21.0 Hz, $P(CH_3)_3$) (one additional aromatic ^{13}C signal is missing, likely due to overlap with C_6D_6). Anal. Calcd for $C_{47}H_{47}CoN_2SP_4$: C, 66.04; H, 5.54; N, 3.28. Found: C, 65.72; H, 5.64: N, 2.92.

X-Ray crystallography procedures.

All operations were performed on a Bruker-Nonius Kappa Apex2 diffractometer, using graphite-monochromated MoKα radiation. All diffractometer manipulations, including data collection, integration, scaling, and absorption corrections were carried out using the Bruker Apex2 software.[50] Preliminary cell constants were obtained from three sets of 12 frames. A fully labelled diagrams and data collection and refinement details are included in the ESI. Further crystallographic details may be found in the accompanying CIF file.

Computational methods.

All calculations were performed using Gaussian09 for the Linux operating system.[51] DFT calculations were carried out using the B3LYP hybrid functional.[52, 53] A mixed basis set was employed, using the LANL2DZ (p, d) double-ζ basis set with effective core potentials for the P, S, and Co atoms[54-57] and Gaussian09's internal LANL2DZ basis set (equivalent to D95V[58]) for C, O, N, and H atoms. Starting from crystallographically determined coordinates, the geometry of **2** was optimized to a minimum. Using modifications of crystallographically determined geometries of similar complexes as the starting point, the geometries of **2***, **3**, and **4** were optimized to minima. Subsequent analytical frequency calculations were used to confirm that no imaginary frequencies were present. A table of XYZ coordinates of all calculated compounds is provided in the ESI.

Conflicts of interest

There are no conflicts to declare.

Acknowledgements

This material is based on work supported by the National Science Foundation under award number CHE-1764170. The Ohio State University Department of Chemistry and Biochemistry and the Sustainable and Resilient Economy program are also gratefully acknowledged for financial support. The authors are also grateful for access to the Brandeis University high-performance computing cluster and the Ohio Supercomputer Center.[59]

Notes and references

1. J. F. Hartwig, *Organotransition Metal Chemistry: From Bonding to Catalysis*, University Science Books, Sausalito, CA, 2010.
2. R. M. Bullock, *Catalysis Without Precious Metals*, Wiley-VCH, Weinheim, 2010.
3. P. Chirik and R. Morris, *Acc. Chem. Res.*, 2015, **48**, 2495-2495.
4. J. R. Khusnutdinova and D. Milstein, *Angew. Chem. Int. Ed.*, 2015, **54**, 12236-12273.
5. J. I. van der Vlugt, *Eur. J. Inorg. Chem.*, 2012, **2012**, 363-375.
6. V. K. K. Praneeth, M. R. Ringenberg and T. R. Ward, *Angew. Chem. Int. Ed.*, 2012, **51**, 10228-10234.
7. V. Lyaskovskyy and B. de Bruin, *ACS Catalysis*, 2012, **2**, 270-279.
8. P. J. Chirik, *Acc. Chem. Res.*, 2015, **48**, 1687-1695.
9. O. R. Luca and R. H. Crabtree, *Chem. Soc. Rev.*, 2013, **42**, 1440-1459.
10. W. Kaim and B. Schwederski, *Coord. Chem. Rev.*, 2010, **254**, 1580-1588.
11. W. I. Dzik, J. I. van der Vlugt, J. N. H. Reek and B. de Bruin, *Angew. Chem. Int. Ed.*, 2011, **50**, 3356-3358.
12. H. Grützmacher, *Angew. Chem. Int. Ed.*, 2008, **47**, 1814-1818.
13. R. H. Morris, *Acc. Chem. Res.*, 2015, **48**, 1494-1502.
14. M. D. Fryzuk, C. D. Montgomery and S. J. Rettig, *Organometallics*, 1991, **10**, 467-473.
15. M. D. Fryzuk, P. A. MacNeil and S. J. Rettig, *J. Am. Chem. Soc.*, 1987, **109**, 2803-2812.
16. T. Ikariya and A. J. Blacker, *Acc. Chem. Res.*, 2007, **40**, 1300-1308.
17. R. Noyori and S. Hashiguchi, *Acc. Chem. Res.*, 1997, **30**, 97-102.
18. L. C. Gregor, C.-H. Chen, C. M. Fafard, L. Fan, C. Guo, B. M. Foxman, D. G. Gusev and O. V. Ozerov, *Dalton Trans.*, 2010, **39**, 3195-3202.
19. A. M. Poitras, S. E. Knight, M. W. Bezpalko, B. M. Foxman and C. M. Thomas, *Angew. Chem. Int. Ed.*, 2018, **57**, 1497-1500.
20. M.-A. M. Hoyle, D. A. Pantazis, H. M. Burton, R. McDonald and L. Rosenberg, *Organometallics*, 2011, **30**, 6458-6465.
21. E. J. Derrah, D. A. Pantazis, R. McDonald and L. Rosenberg, *Organometallics*, 2007, **26**, 1473-1482.

22. M. D. Fryzuk and K. Bhangu, *J. Am. Chem. Soc.*, 1988, **110**, 961-963.
23. L. Dahlenburg, N. Höck and H. Berke, *Chem. Ber.*, 1988, **121**, 2083-2093.
24. D. M. Roddick, B. D. Santarsiero and J. E. Bercaw, *J. Am. Chem. Soc.*, 1985, **107**, 4670-4678.
25. D. M. Stefanescu, H. F. Yuen, D. S. Glueck, J. A. Golen, L. N. Zakharov, C. D. Incarvito and A. L. Rheingold, *Inorg. Chem.*, 2003, **42**, 8891-8901.
26. M. M. Hossain, H.-M. Lin and S.-G. Shyu, *Organometallics*, 2003, **22**, 3262-3270.
27. M. A. Esteruelas, A. M. López, J. I. Tolosa and N. Vela, *Organometallics*, 2000, **19**, 4650-4652.
28. R. Weinand and H. Werner, *Chem. Ber.*, 1986, **119**, 2055-2058.
29. K. Jörg, W. Malisch, W. Reich, A. Meyer and U. Schubert, *Angew. Chem.*, 1986, **98**, 103-104.
30. S. Oh and Y. Lee, *Organometallics*, 2016, **35**, 1586-1592.
31. S. Oh, S. Kim, D. Lee, J. Gwak and Y. Lee, *Inorg. Chem.*, 2016, **55**, 12863-12871.
32. Y.-E. Kim, S. Oh, S. Kim, O. Kim, J. Kim, S. W. Han and Y. Lee, *J. Am. Chem. Soc.*, 2015, **137**, 4280-4283.
33. H.-U. Reisacher, E. N. Duesler and R. T. Paine, *J. Organomet. Chem.*, 1998, **564**, 13-20.
34. L. Rosenberg, *Coord. Chem. Rev.*, 2012, **256**, 606-626.
35. D. Gudat, *Coord. Chem. Rev.*, 1997, **163**, 71-106.
36. D. Gudat, *Eur. J. Inorg. Chem.*, 1998, **1998**, 1087-1094.
37. R. K. Bansal and D. Gudat, in *Phosphorus Heterocycles II*, Springer Berlin / Heidelberg, vol. 21, pp. 63-102.
38. H. Nakazawa, *J. Organomet. Chem.*, 2000, **611**, 349-363.
39. H. Nakazawa, in *Adv. Organomet. Chem.*, Academic Press, 2004, vol. Volume 50, pp. 107-143.
40. B. Pan, M. W. Bezpalko, B. M. Foxman and C. M. Thomas, *Organometallics*, 2011, **30**, 5560-5563.
41. B. Pan, Z. Xu, M. W. Bezpalko, B. M. Foxman and C. M. Thomas, *Inorg. Chem.*, 2012, **51**, 4170-4179.
42. M. W. Bezpalko, B. M. Foxman and C. M. Thomas, *Inorg. Chem.*, 2015, **54**, 8717-8726.
43. M. W. Bezpalko, A. M. Poitras, B. M. Foxman and C. M. Thomas, *Inorg. Chem.*, 2017, **56**, 503-510.
44. B. Stadelmann, J. Bender, D. Forster, W. Frey, M. Nieger and D. Gudat, *Dalton Trans.*, 2015, **44**, 6023-6031.
45. M. Gediga, C. M. Feil, S. H. Schlindwein, J. Bender, M. Nieger and D. Gudat, *Chem. Eur. J.*, 2017, **23**, 11560-11569.
46. G. S. Day, B. Pan, D. L. Kellenberger, B. M. Foxman and C. M. Thomas, *Chem. Commun.*, 2011, **47**, 3634-3636.
47. B. Pan, M. W. Bezpalko, B. M. Foxman and C. M. Thomas, *Dalton Trans.*, 2012, **41**, 9083-9090.
48. A. W. Addison, T. N. Rao, J. Reedijk, J. van Rijn and G. C. Verschoor, *J. Chem. Soc., Dalton Trans.*, 1984, **0**, 1349-1356.
49. K. P. Kepp, *Inorg. Chem.*, 2016, **55**, 9461-9470.
50. , *Apex 2: Version 2 User Manual, M86-E01078*, Bruker Analytical X-ray Systems, Madison, WI, 2006.
51. M. J. Frisch, G. W. Trucks, H. B. Schlegel, G. E. Scuseria, M. A. Robb, J. R. Cheeseman, G. Scalmani, V. Barone, B. Mennucci and G. A. Petersson, *Journal*, et al. (see ESI for full reference), 2009, Gaussian 09, Revision A. 1.
52. A. D. Becke, *J. Chem. Phys.*, 1993, **98**, 5648-5652.
53. C. Lee, W. Yang and R. G. Parr, *Physical Review B*, 1988, **37**, 785-789.
54. L. E. Roy, P. J. Hay and R. L. Martin, *J. Chem. Theory Comput.*, 2008, **4**, 1029-1031.
55. P. J. Hay and W. R. Wadt, *J. Chem. Phys.*, 1985, **82**, 284-298.
56. P. J. Hay and W. R. Wadt, *J. Chem. Phys.*, 1985, **82**, 299-310.
57. P. J. Hay and W. R. Wadt, *J. Chem. Phys.*, 1985, **82**, 270-283.
58. T. H. Dunning, Hay, P. J., in: H.F. Schaefer (Ed.), Modern Theoretical Chemistry, Plenum, New York, 1976, pp. 1–28.
59. *Ohio Supercomputer Center*, Columbus, OH, 1987.

A cobalt N-heterocyclic phosphide complex is shown to cleave element-hydrogen bonds via a metal-phosphorus ligand cooperative pathway.